Analytica Chimica Acta xxx (2016) 1–7

Contents lists available at ScienceDirect

Analytica Chimica Acta

journal homepage: www.elsevier.com/locate/aca

One-step synthesis of DNA functionalized cadmium-free quantum dots and its application in FRET-based protein sensing

Cuiling Zhang [a, **], Caiping Ding [a], Guohua Zhou [b], Qin Xue [a], Yuezhong Xian [a, *]

[a] Department of Chemistry, School of Chemistry and Molecular Engineering, East China Normal University, Shanghai 200241, China
[b] School of Chemistry and Chemical Engineering, Lingnan Normal University, Zhanjiang, 524048, China

HIGHLIGHTS

- The stable and cadmium-free DNA functionalized ZnS:Mn^{2+} QDs were successfully synthesized through a facile one-step route.
- We constructed a novel FRET system based on one-step synthesized DNA-ZnS:Mn^{2+} QDs (donor) and WS_2 nanosheets (acceptor).
- The FRET-based strategy was applied for the detection of streptavidin and folate receptor by combining TPSMLD and Exo III.

GRAPHICAL ABSTRACT

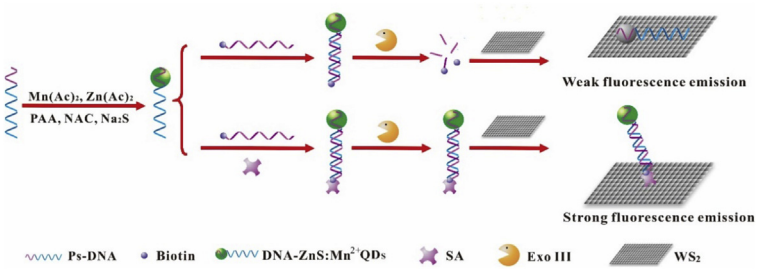

ARTICLE INFO

Article history:
Received 11 November 2016
Accepted 13 December 2016
Available online xxx

Keywords:
Biosensor
FRET
Quantum dots
WS_2
Terminal protection of small-molecule linked DNA

ABSTRACT

DNA functionalized quantum dots (QDs) are promising nanoprobes for the fluorescence resonance energy transfer (FRET)-based biosensing. Herein, cadmium-free DNA functionalized Mn-doped ZnS (DNA-ZnS:Mn^{2+}) QDs were successfully synthesized by one-step route. As-synthesized QDs show excellent photo-stability with the help of PAA and DNA. Then, we constructed a novel FRET model based on the QDs and WS_2 nanosheets as the energy donor-acceptor pairs, which was successfully applied for the protein detection through the terminal protection of small molecule-linked DNA assay. This work not only explores the potential bioapplication of the DNA-ZnS:Mn^{2+} QDs, but also provides a platform for the investigation of small molecule-protein interaction.

1. Introduction

Quantum dots (QDs) have been widely used in various applications in the past decades, because of their unique optical properties relative to the traditional organic dyes [1–3]. From the perspective of the science and technology, in most cases, it is necessary and desirable to synthesize the surface-functionalized QDs, particularly for the DNA functionalized QDs [4,5]. The classical approaches for preparing DNA functionalized QDs are electrostatic attraction, biotin–avidin coupling and covalent bonding through amino/carboxyl groups [6–9]. However, these methods still have some disadvantages, such as non-specific adsorption, high cost, decreased fluorescence and multi-step process. One-step synthesis of DNA functionalized QDs was thus developed by using the phosphorothiolate phosphate DNA (Ps-DNA) as ligands during the preparation of CdTe QDs [10–13]. However, a major concern for the DNA functionalized CdTe QDs is their potential toxicity due to the existence of cadmium element. In order to address this issue,

* Corresponding author.
** Corresponding author.
E-mail addresses: clzhang@chem.ecnu.edu.cn (C. Zhang), yzxian@chem.ecnu.edu.cn (Y. Xian).

http://dx.doi.org/10.1016/j.aca.2016.12.024
0003-2670/

we have synthesized Zn-doped DNA functionalized CdTe QDs to reduce the toxicity of QDs stemmed from cadmium [14]. Despite the great success of one-step synthesis of DNA functionalized QDs, it is necessary to solve the problem of the intrinsic toxicity from the cadmium source, which limits the biological applicability of these DNA functionalized QDs. In light of this, exploring a facile approach for synthesizing cadmium-free DNA functionalized QDs is crucial to meet the requirement of biosensing and bioimaging.

Recently, as one of the emerging two-dimensional (2D) nanomaterials, transition metal dichalcogenides, such as WS_2, have attracted great interest due to their unique electrical and mechanical properties, as well as their potential applications in the fields of catalytic reactions, solar cells, lithium ion batteries, and field-effect transistors [15–19]. Most recently, WS_2 nanosheets were used in the biosensing because of its differential affinity towards single-stranded DNA (ssDNA) and double-stranded DNA (dsDNA) [20–25]. These assays were utilized for fluorescence resonance energy transfer (FRET) between organic dyes as energy donors and WS_2 as the energy acceptor. Compared with conventional organic dyes as energy donors, QDs are promising candidates in FRET-based assays, since they possess several advantages, including high quantum yield, excellent photostability, size-dependent fluorescence spectra and tunable absorption and emission [26]. However, the relatively low quenching efficiency of the fluorescence of QDs using organic dyes as quenchers is a major problem for the QDs-based FRET [27]. Although gold nanoparticles and carbon nanomaterials have given high quenching efficiency [28], the former needs to be labeled and the latter has difficulty in the large scale synthesis compared to WS_2.

Mn-doped ZnS QDs is one of the most extensively investigated cadmium-free fluorescent materials. Herein, we prepared DNA functionalized Mn-doped ZnS (DNA-ZnS:Mn^{2+}) QDs by one-step synthesis for the first time, and then, the as-prepared QDs and WS_2 nanosheets were utilized as novel energy donor–acceptor pairs to construct the FRET-based assay system. Recently, as one of the most commonly used methods for protein detection, terminal protection of small molecule linked DNA (TPSMLD) has attracted considerable attention [29–32]. It is based on the fact that the small molecule-linked ssDNA can be protected from degradation by exonuclease I once the small molecule binds to the target protein [28]. Taking the biotin-streptavidin (SA) and folate-folate receptor (FR) interactions as models, the as-constructed FRET system was further developed for protein sensing based on the principle of TPSMLD.

2. Materials and methods

2.1. Chemicals and reagents

N-acetylcysteine (NAC), poly(acrylic acid) (PAA, MW = 2000), $Mn(Ac)_2{\cdot}4H_2O$, $Zn(Ac)_2$, $Na_2S{\cdot}9H_2O$ were purchased from Aladdin Industrial Corporation (Shanghai, China). SA was purchased from Amresco (USA). Exonuclease III (Exo III) was purchased from Takara Biotechnology Co., Ltd. (Dalian, China). FR was obtained from Biosynthesis Biotechnology CO., Ltd. (Beijing, China). Albumin (BSA) was purchased from Sigma-Aldrich (St. Louis, MO, USA). Thrombin was purchased from Wenhan Technology Development Co., Ltd. (Hubei, China). The other chemicals not mentioned here were of analytical-regent grade or better. Sodium dodecyl sulfate polyacrylamide gel electrophoresis (SDS-PAGE) gel preparation kit was purchased from Solaibao Biological Technology Co., Ltd. (Shanghai, China). SYBR green 1 and Immunoglobulin G (IgG), and all oligonucleotides with different sequences were purchased by Sangon Biotechnology Co., Ltd. (Shanghai, China).

Ps-DNA: 5′-TATATGGATGATGTGGTATTAAAAA*G*G*G*G*G*G *G*G*G*G-3’ (* indicates the phosphorothioate linkage)
Biotin-DNA: 5′-AATACCACATCATCCATATA-biotin-3′
Folate-DNA: 5′-AATACCACATCATCCATATA-FA-3′
Complement DNA (C_{DNA}): 5′-AATACCACATCATCCATATA-3′

2.2. Characterization

Transmission electron microscope (TEM), high resolution TEM (HRTEM) and selected area electron diffraction (SAED) images were performed using HT-7700 TEM (Japan). Atomic force microscope (AFM) image was acquired by a tapping mode in air using Multimode 8 atomic force microscope (VEECO, USA). X- ray diffraction (XRD) was measured on a Bruker D8 advance X-ray diffractometer (Germany). UV–vis absorption spectra were taken using a Shimadzu UV-2550 spectrophotometer (Japan). Fluorescence spectra were measured on a Hitachi F-7000 fluorescence spectrophotometer (Japan). The Energy-dispersive spectrum (EDS) was recorded with a scanning electron microscopy (SEM) (FEI Quanta 200). Dynamic light scattering (DLS) and zeta (ζ) potential measurements were performed on a Zeta sizer Nano ZS90 nanoparticle size and ζ potential analyzer (Malvern, U.K.). PAGE analysis was obtained from EPS 300 electrophoresis apparatus (Tanon, Shanghai) with 120 V for 90 min. A Spectro Genesisi FEE inductivity coupled plasma optical emission spectrometer (ICP-OES) (Thermo Electron Corporation, USA) was used for the determination of Zn concentration in solution.

2.3. Preparation of DNA-ZnS:Mn^{2+} QDs

$Zn(Ac)_2$ (5.75 mM), $Mn(Ac)_2{\cdot}4H_2O$ (0.17 mM), PAA (4.5 mg) and NAC (6.8 mM) were added into a three-necked flask containing 10 mL deionized water. Then, 625 μL of 0.1 M Na_2S was injected into the solution and adjusted to pH = 9 with NaOH. The reaction solution was stirred for 10 min, and then DNA solution (20 μM) was added into the above-mentioned solution. The mixture was incubated at 90 °C for 2 h and gradually cooled to the room temperature. The final solution was further purified by ultrafiltration (an Amicon Ultra-4 centrifugal filter device with a MW cut off of 30 kDa).

2.4. Synthesis of WS_2 nanosheets

Briefly, WS_2 powder (160 mg) and CTAB (80 mg) were added to a 250 mL beaker containing 160 mL of deionized water and the mixture was sonicated for 3 h. Then, the dark green dispersion was centrifuged at 3500 rpm for 10 min to remove large-size masses. The supernatant was washed with water by centrifugation at 12000 rpm for 10 min. The as-obtained supernatant was further centrifuged at 16000 rpm for 5 min to remove the redundant CTAB. Then WS_2 nanosheets were dispersed in water and stored in the refrigerator for further use.

2.5. Procedure for the detection of SA

7.5 μL of 1 mg/mL DNA-ZnS:Mn^{2+} QDs, 12.5 μL of 10 μM biotin-DNA and different concentrations of SA in PBS buffer (0.02 M, pH = 7.4, containing 50 mM NaCl and 10 mM $MgCl_2$) were kept at 37 °C for 45 min. Then 80 U Exo III was added into the hybridization solution and the mixtures were kept at 37 °C for another 45 min with gentle agitation. After that, 18 μL of 2 mg/mL WS_2 were added with a final volume of 500 μL and incubated for 1 min before measurement. Finally, the fluorescence intensity of the incubated solution was measured at 575 nm with excitation at 330 nm.

Please cite this article in press as: C. Zhang, et al., One-step synthesis of DNA functionalized cadmium-free quantum dots and its application in FRET-based protein sensing, Analytica Chimica Acta (2016), http://dx.doi.org/10.1016/j.aca.2016.12.024

3. Results and discussion

3.1. Synthesis and characterization of DNA-ZnS:Mn^{2+} QDs and WS_2 nanosheets

As shown in Scheme 1, DNA-ZnS:Mn^{2+} QDs were synthesized by one-pot route, in which Ps-DNA [10] (two domains: phosphorothiolates binding with the ZnS:Mn^{2+} QDs surface and recognition sequence for targeting biomolecular) and NAC were used as the coligand. Fig. 1A shows the TEM image of DNA-ZnS:Mn^{2+} QDs, and the average diameter is ~3.8 nm based on the size histograms (Fig. 1B). According to HRTEM (inset in the Fig. 1A), QDs is highly crystalline. The XRD pattern displays that these nanoparticles possess a cubic zinc blende structure [33] (Fig. 1C). The results preliminarily indicate the successful synthesis of DNA-ZnS:Mn^{2+} QDs. We further investigated the effect of surface ligands on the hydrodynamic size and surface charge of the QDs. As shown in Fig. S1A, the hydrodynamic size of the ZnS:Mn^{2+} -QDs (only NAC), PAA-ZnS:Mn^{2+} QDs (NAC and PAA) and DNA-ZnS:Mn^{2+} QDs (NAC, PAA and DNA) were 6.11, 8.38 and 11.19 nm, respectively. The difference in diameter could be attributed to the different surface species of as-prepared QDs in aqueous phase. Because of the presence of DNA and PAA, it could increase the diameter of QDs. As shown in Fig. S1B, zeta-potential measurements of the ZnS:Mn^{2+}-QDs, PAA-ZnS:Mn^{2+} QDs and DNA-ZnS:Mn^{2+} QDs were −21.7, −30.8 and −45.3 mV, respectively, indicating the surface charge were dominated by negative NAC, PAA and DNA on the surface of QDs.

WS_2 were prepared through the ultrasonication in the presence of CTAB which can stabilize the nanomaterials against aggregation [34,35]. Bulk WS_2 can be easily exfoliated to lamellar forms under the help of CTAB (shown in Fig. S2A). In addition, the SAED patterns demonstrate that the as-prepared are polycrystalline (inset in the Fig. S2A). The thickness of the WS_2 nanosheets is less than 3 nm (Figs. S2C and D), indicating its few-layered nanostructure based on the height of monolayer about 0.8–1.0 nm [36]. The elemental composition of the WS_2 was identified by EDS, and strong peaks of W and S were observed (Fig. S2B). The molar ratio of W:S is calculated as 37.34: 62.66 (≈1: 1.7) based on the peak intensities (inserted table in Fig. S2B), thereby confirming the desired stoichiometry of the nanosheets.

3.2. Optical propreties of DNA-ZnS:Mn^{2+} QDs

Fig. 2A shows the UV–Vis absorption and fluorescence spectra of DNA-ZnS:Mn^{2+} QDs, and the corresponding controls are PAA modified ZnS:Mn^{2+} QDs (PAA-ZnS:Mn^{2+} QDs) prepared under the same condition. It can be easily observed that DNA-ZnS:Mn^{2+} QDs display a clear absorption peak at 260 nm, suggesting the existence of DNA on their surfaces. The fluorescence spectrum of DNA-ZnS:Mn^{2+} QDs exhibits little red-shift (approximately 3 nm) and relatively strong fluorescence intensity compared with PAA-ZnS:Mn^{2+} QDs. This phenomenon may be attributed that nucleic acids can make up the surface defects of QDs and improve the fluorescence feature of the QDs [37]. Fig. 2B shows the photostability of as-prepared QDs. All colloids were irradiated under 365 nm for 2.5 h. The fluorescence intensities of DNA-ZnS:Mn^{2+} QDs (curve a) retain around 90% of the initial value, however, for PAA-ZnS:Mn^{2+} QDs and ZnS:Mn^{2+} QDs, only about 63% and 42% fluorescence intensities were reserved, respectively. Small molecule ligand (NAC) was easily detached from the surface of QDs when their surroundings were changed [38]. Polymeric coatings are effective on preventing aggregation for colloidal nanoparticles because of the steric hindrance. As a type of water-soluble polymers, PAA was thus utilized as the electrostatic stabilizer to improve the stability of QDs [39,40]. DNA can also improve photostability of the QDs by decreasing surface defects [14].

3.3. Confirmation of DNA on the surface of DNA-ZnS:Mn^{2+} QDs

SYBR green 1 is one of the most sensitive stains for probing dsDNA because of its preferential binding to dsDNA with high fluorescence and low fluorescence in the presence of ssDNA. It was used to test the DNA targeting on the surface of DNA-ZnS:Mn^{2+} QDs (Fig. 2C). When DNA-ZnS:Mn^{2+} QDs were incubated with C_{DNA} and SYBR green 1, the fluorescence peak at 520 nm from SYBR green 1 was observed. Under other conditions, the no or low fluorescent signal at 520 nm was observed, including only SYBR green 1, C_{DNA} + SYBR green 1, DNA-ZnS:Mn^{2+} QDs + SYBR green 1. It should be noted that the broad peak of the mixture of DNA-ZnS:Mn^{2+} QDs and SYBR green 1 was attributed to the fluorescence of QDs. The experiment data show that DNA has been successfully grated on the surface of QDs. Gel electrophoresis analysis was also employed to prove DNA on the surface of QDs. As shown in Fig. S3, the migration shift of DNA-ZnS:Mn^{2+} QDs (lane a) was decreased compared to that of C_{DNA} (lane b) in the presence of SYBR Green I fluorescent dye due to the molecular weight increase of DNA-ZnS:Mn^{2+} QDs. Lane c shows a clear fluorescent band, revealing that dsDNA was obtained through the hybridization of the DNA-ZnS:Mn^{2+} QDs and C_{DNA}. The phenomenon further display DNA has been successfully grafted on

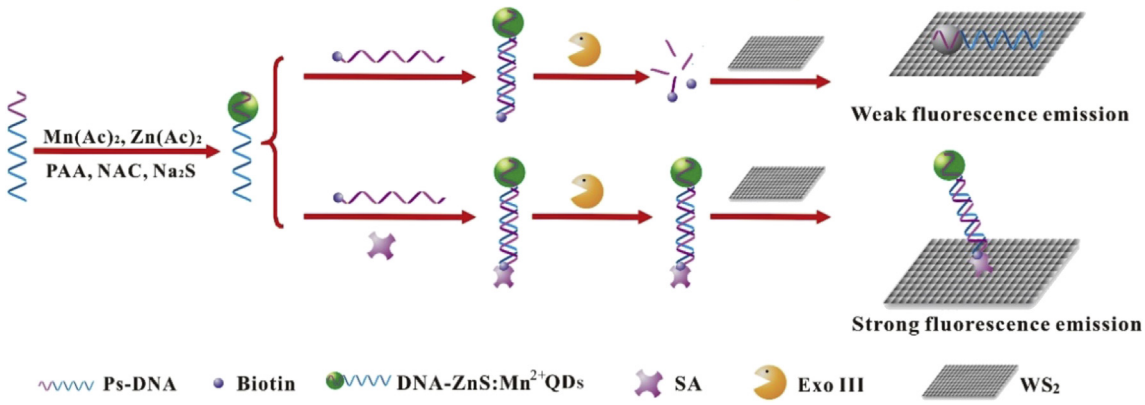

Scheme 1. Scheme illustration of the one-pot synthesized DNA-ZnS:Mn^{2+} QDs and the principle of biosensor for SA detection based on the FRET between the DNA-ZnS:Mn^{2+} QDs and WS_2.

Please cite this article in press as: C. Zhang, et al., One-step synthesis of DNA functionalized cadmium-free quantum dots and its application in FRET-based protein sensing, Analytica Chimica Acta (2016), http://dx.doi.org/10.1016/j.aca.2016.12.024

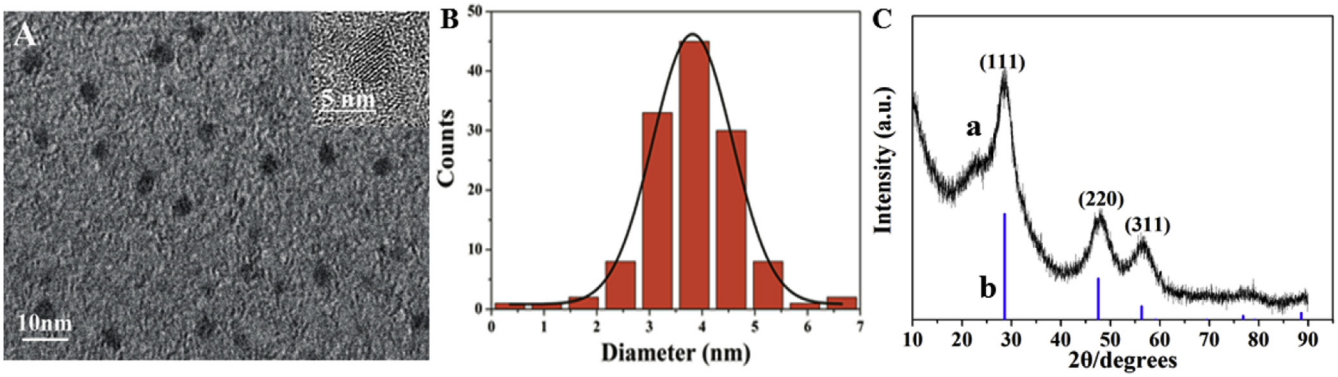

Fig. 1. (A) TEM and HRTEM images, (B) the corresponding size distribution, (C) the XRD of the as-synthesized DNA-ZnS:Mn^{2+} QDs (black line) and the standard pattern of ZnS QDs (blue line, JCPDs card 12-0688). (For interpretation of the references to colour in this figure legend, the reader is referred to the web version of this article.)

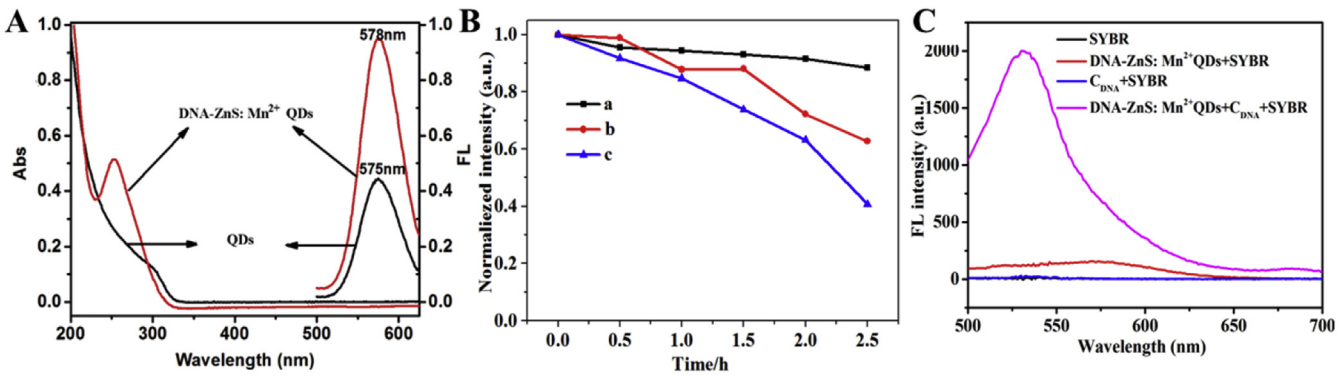

Fig. 2. (A) The UV–vis and fluorescence spectra of DNA-ZnS:Mn^{2+} QDs (red line) and PAA-ZnS:Mn^{2+} QDs (black line) in the same synthesis condition; (B) the photostability of the DNA-ZnS:Mn^{2+} QDs (a), PAA-ZnS:Mn^{2+} QDs (b) and ZnS:Mn^{2+} QDs (c); (C) fluorescence spectra of DNA-ZnS:Mn^{2+} QDs and SYBR green 1 before and after interaction, SYBR (black line, coinciding with the blue line), DNA-ZnS:Mn^{2+} QDs + SYBR (red line), C_{DNA} + SYBR (blue line), DNA-ZnS:Mn^{2+} QDs + C_{DNA} + SYBR (purple line). (For interpretation of the references to colour in this figure legend, the reader is referred to the web version of this article.)

the surface of QDs *via* one-step synthesis.

3.4. Principle of the sensing platform based on the FRET between WS2 DNA-ZnS:Mn^{2+} QDs and WS_2 nanosheets

A protein biosensor was developed by using DNA-ZnS:Mn^{2+} QDs as the energy donor and WS_2 as the energy acceptor. Biotin-SA was chosen as the model of protein sensing. As shown in Scheme 1, in the absence of SA, DNA-ZnS:Mn^{2+} QDs were hybridized with biotin-DNA to obtain dsDNA. When Exo III was added into this system, the biotin-DNA was hydrolyzed for the stepwise removal of mononucleotides from the 3′ -hydroxyl termini of dsDNA, releasing DNA-ZnS:Mn^{2+} QDs into solution. After incubation with WS_2 nanosheets, DNA-ZnS:Mn^{2+} QDs were absorbed on the surface of WS_2 due to their stronger affinity towards ssDNA than that of dsDNA, which would lead to the fluorescence quenching of QDs. However, upon the addition of SA, the specific binding of SA to biotin could avoid the degradation of biotin-DNA in dsDNA by Exo III based on the principle of TPSMLD. Consequently, QDs with dsDNA could be kept far away from the surface of WS_2, making QDs retain their fluorescence. Therefore, protein detection could be easily realized based on the DNA-ZnS:Mn^{2+} QDs -WS_2 nanoarchitecture with the aid of TPSMLD.

3.5. Feasible experiment of the biosensor

To verify this design, the feasible experiment was carried out (Fig. 3). Firstly, the original fluorescence intensity of DNA-ZnS:Mn^{2+} QDs (curve a) was dramatically decreased to 14.4% in the presence of WS_2 (curve b), suggesting the adsorption of QDs on WS_2 and an impressive fluorescence quenching efficiency of WS_2. In the presence of WS_2 and biotin-DNA, a remarkable fluorescence recovery is occurred because of the formation of dsDNA (curve c). However, the

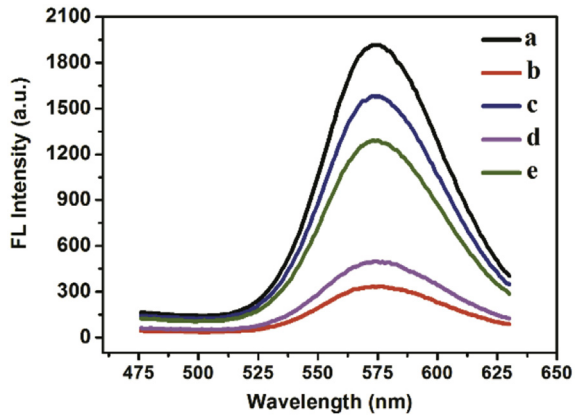

Fig. 3. Fluorescence spectra of the DNA-ZnS:Mn^{2+} QDs (a) in PBS buffer, with (b) WS_2, (c) biotin-DNA + WS_2, (d) biotin-DNA + WS_2 + Exo III, (e) biotin-DNA + WS_2 + Exo III + SA. (DNA-ZnS:Mn^{2+} QDs: 15 μg/mL, Biotin-DNA: 300 nM, WS_2: 72 μg/mL, Exo III: 80 U, SA: 300 ng/mL. Excitation: 330 nm).

Please cite this article in press as: C. Zhang, et al., One-step synthesis of DNA functionalized cadmium-free quantum dots and its application in FRET-based protein sensing, Analytica Chimica Acta (2016), http://dx.doi.org/10.1016/j.aca.2016.12.024

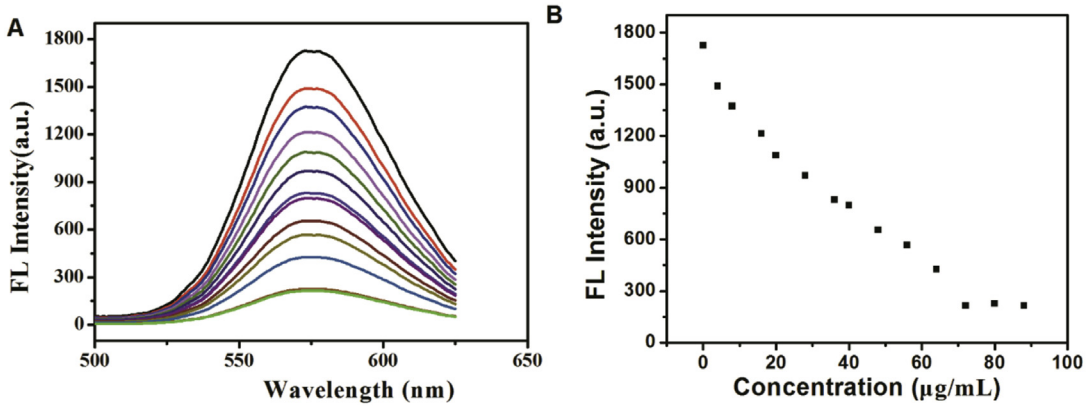

Fig. 4. (A) Fluorescence spectra of DNA-ZnS:Mn^{2+} QDs in the presence of various concentrations of WS_2 in PBS buffer; (B) the linear curve of fluorescent intensities versus concentrations of WS_2.

recovery of fluorescence signal was not observed under the condition of coexistence of Exo III (curve d), implying the digestion of dsDNA by Exo III and the fluorescence quenching of QDs by WS_2. Upon the addition of biotin-DNA, Exo III and SA, an intense fluorescence signal was recorded owing to the specific interaction between biotin and SA (curve e), which could protect biotin-dsDNA from the Exo III-catalyzed degradation. The experimental data demonstrate that it is feasible for the detection of SA by terminal protection of biotin-linked DNA through DNA-ZnS:Mn^{2+} QDs - WS_2 nanoarchitecture.

3.6. Optimization of the experimental parameters

To further optimize the performance of the biosensing system, The effect of the concentration of WS_2 on the DNA-ZnS:Mn^{2+} QDs fluorescence was investigated. As shown in Fig. 4, the fluorescence intensity decreased dramatically with an increase in WS_2 concentration from 0 to 88 μg/mL. About 88% original fluorescence intensity was quenched with a WS_2 concentration of 72 μg/mL. Consequently, 72 μg/mL WS_2 was chosen as the optimized concentration for bioassay. And then, we also optimize the reaction time between DNA-ZnS:Mn^{2+} QDs and WS_2, as shown in Fig. S4, the fluorescence of DNA-ZnS:Mn^{2+} QDs couled be quenched by WS_2 to 88% within 1 min. The results exhibit the high quenching efficiency of WS_2.

Subsequently, the concentrations of biotin-DNA and Exo III were further optimized. The fluorescence signal of QDs was improved with the increasing concentration of biotin-DNA from 0 to 250 nM while the concentrations of DNA-ZnS:Mn^{2+} QDs and WS_2 were fixed (Fig. S5). At higher concentration, the fluorescence intensity was almost unchanged. In addition, the amount of Exo III in this assay also affects the sensitivity of the biosensor. As shown in Fig. S6, when the concentration of DNA-ZnS:Mn^{2+} QDs, WS_2 and biotin-DNA were fixed, the fluorescence intensity was reduced with the increasing concentration of Exo III and reached a plateau with 80 U of Exo III. Therefore, 250 nM of biotin-DNA and 80 U of Exo III were selected for SA assay.

3.7. The FRET-based biosensor for SA detection

Fig. 5A depicts the fluorescence responses of DNA-ZnS: Mn^{2+} QDs for different SA concentrations. The fluorescence signals increase intensely with the increasing concentration of SA and tend to reach saturation at high SA concentration (Fig. 5B). There is a good linear relationship between the fluorescence intensities and the concentration of SA in the range of 5–150 ng/mL with the linear equation $y = 5.2\ x + 401.4$ ($R^2 = 0.9976$) (inset of Fig. 5B). The detection limit was calculated as 2.8 ng/mL ($3S_b/S$, where S_b is the standard deviation for the blank solution (n = 11) and S is the slope for the range of linearity), which is comparable to the reported

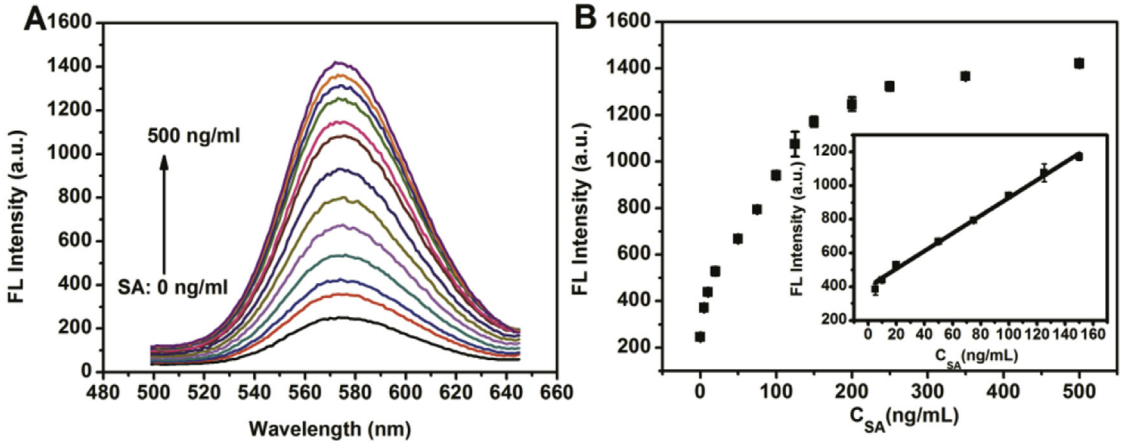

Fig. 5. (A) Fluorescence spectra of the DNA-ZnS:Mn^{2+} QDs upon the addition of increasing concentrations of SA (0–500 ng/mL); (B) Calibration curve for SA detection (inset, linear relationship between the fluorescence increase intensity and the SA concentration (5, 10, 20, 50, 75, 100, 125, and 150 ng/mL). DNA-ZnS:Mn^{2+} QDs: 15 μg/mL, Exo III: 80 U, WS_2: 72 μg/mL. Excitation: 330 nm.

Please cite this article in press as: C. Zhang, et al., One-step synthesis of DNA functionalized cadmium-free quantum dots and its application in FRET-based protein sensing, Analytica Chimica Acta (2016), http://dx.doi.org/10.1016/j.aca.2016.12.024

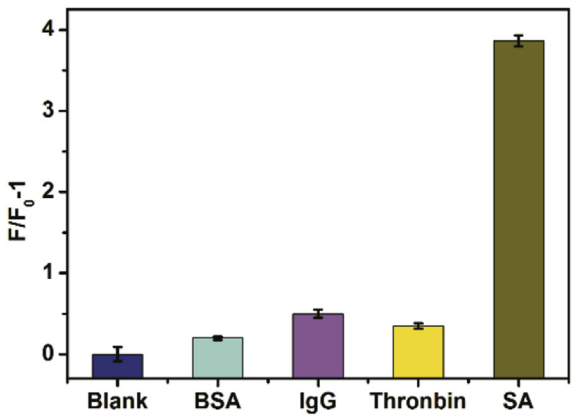

Fig. 6. Relative fluorescence intensities of the WS_2-based assay in the presence of different proteins: blank control (without SA), BSA: 150 ng/mL, IgG: 150 ng/mL, Thrombin: 150 ng/mL, SA: 150 ng/mL (F_0 and F are the fluorescence intensities in the absence and presence of proteins, respectively) Excitation: 330 nm.

florescent assay [41,42]. The good reproducibility of the assay was also shown according to the standard deviations from independent measurement (n = 3) (Fig. 5B).

3.8. Specificity and interference of the assay towards SA

To verify the specificity of the biosensor, some other proteins were examined, including BSA, IgG, and thrombin. Fig. 6 displays the fluorescence of the FRET-based system, and few changes are observed for BSA, IgG and thrombin, respectively, except for SA. The phenomenon is attributed to the specificity between biotin and SA. Furthermore, the performance of the biosensor for complex system was further evaluated. As shown in Fig. S7, the response of the biosensing system for SA is almost the same as that of the mixture of SA with other proteins including BSA and IgG. These experimental data clearly show that the selectivity of the biosensor is very well and has potential application for protein detection in complicated system.

3.9. The FRET-based biosensor for FR detection

To validate the expanded application of our sensing platform, we have also used this method to detect FR by simply changing the small molecule (biotin) to folate. As shown in Fig. 7A, there is a good linear relationship between the fluorescence intensity and the concentration of FR as well. The calibration curve for FR detection is shown in Fig. 7B, and the linear range is from 5 to 325 ng/mL with linear equation $y = 2.45\,x + 248.6$ (inset of Fig. 7B), where y is the fluorescence intensity of DNA-ZnS:Mn^{2+} QDs at 575 nm and x is the concentration of FR (regression coefficient $R^2 = 0.9954$). The detection limit is estimated to be 1.02 ng/mL. It clearly shows that the DNA-ZnS:Mn^{2+} QDs - WS_2 nanoarchitecture can be used to detect other proteins by changing the small molecule at the terminus of DNA. It is a versatile and general platform for protein detection and suitable for the investigation of small molecule-protein interaction.

3.10. Specificity and interference of the assay towards FR

We further investigated the specificity of the folate-FR model. BSA, IgG, thrombin were added into the reaction system with the same concentration of FR, respectively. As shown in Fig. S8A, low fluorescence intensity was observed in the presence of BSA, IgG, thrombin, which was slightly higher than that in the blank sample. Whereas, a significant increase of fluorescence intensity was measured with adding into FR. The results displayed that the biosensing platform was also suitable for the folate-FR model. In addition, we also evaluated the applicability of the biosensor when the protein and mixture of protein were present (Fig. S8B). It had obviously shown the strong anti-interference capability of the assay.

4. Conclusions

In summary, a facile and one-step approach was developed to synthesize DNA-ZnS:Mn^{2+} QDs. The QDs are cadmium-free and can deracinate the toxicity from heavy metal ions. Importantly, the photostability of QDs have been greatly improved with the help of DNA and PAA. Then, the as-prepared QDs and WS_2 nanosheets were utilized as energy donor-acceptor pairs for the first time to detect protein based on TPSMLD. WS_2 nanosheets exhibited high quenching efficiency towards the fluorescence of QDs. Taking the biotin-SA system as a model, the DNA-ZnS:Mn^{2+} QDs - WS_2 nanoarchitecture was successfully developed for the SA detection in the range of 5–150 ng/mL with a detection limit of 2.8 ng/mL. Furthermore, the nanosensor could also be applied to evaluate the interaction of other small molecule with protein (FR and folate).

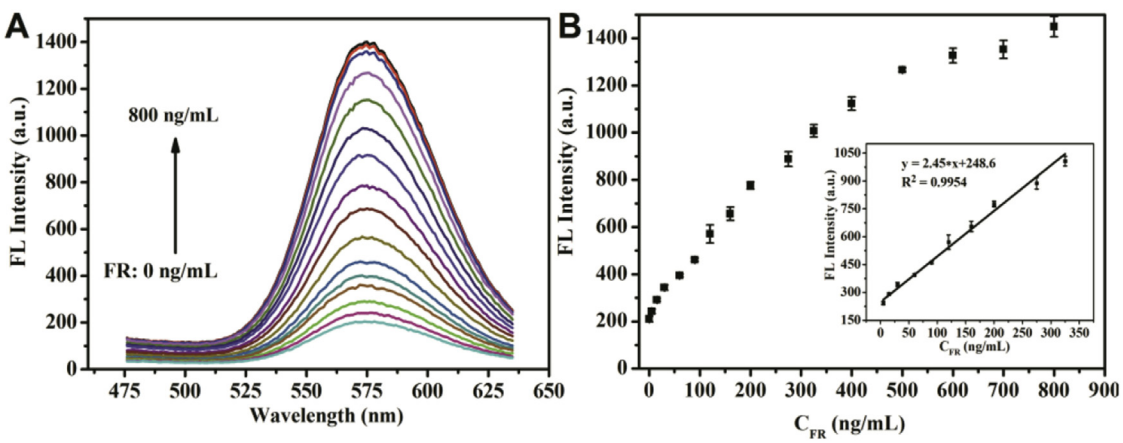

Fig. 7. (A) Fluorescence spectra of the DNA-ZnS:Mn^{2+} QDs upon the addition of increasing concentrations of FR (0–800 ng/mL); (B) Calibration curve for FR detection (inset, linear relationship between the fluorescence increase intensity and the FR concentration (5, 15, 30, 60, 90, 120, 160, 200, 275 and 325 ng/mL). DNA-ZnS:Mn^{2+} QDs: 15 μg/mL, Exo III: 80 U, WS_2: 72 μg/mL. Excitation: 330 nm.

Please cite this article in press as: C. Zhang, et al., One-step synthesis of DNA functionalized cadmium-free quantum dots and its application in FRET-based protein sensing, Analytica Chimica Acta (2016), http://dx.doi.org/10.1016/j.aca.2016.12.024

The DNA terminal protection and the novel energy donor-acceptor pairs for the protein-small molecule interaction show great potential in biological applications.

Acknowledgements

This work was financially supported from the National Natural Science Foundation of China (21605050, 21606149, 21605074), Postdoctoral Science Foundation of China (2015M570349, 2016M591678) and the Shanghai Natural Science Foundation (15ZR1411600).

Appendix A. Supplementary data

Supplementary data related to this article can be found at http://dx.doi.org/10.1016/j.aca.2016.12.024.

References

[1] M. Bruchez, M. Moronne, P. Gin, S. Weiss, A.P. Alivisatos, Semiconductor nanocrystals as fluorescent biological labels, Science 281 (1998) 2013–2016.
[2] W.C.W. Chan, S. Nie, Quantum dot bioconjugates for ultrasensitive nonisotopic detection, Science 281 (1998) 2016–2018.
[3] K.D. Wegner, N. Hildebrandt, Quantum dots: bright and versatile in vitro and in vivo fluorescence imaging biosensors, Chem. Soc. Rev. 44 (2015) 4792–4834.
[4] J.B. Blanco-Canosa, M. Wu, K. Susumu, E. Petryayeva, T.L. Jennings, P.E. Dawson, W.R. Algar, I.L. Medintz, Recent progress in the bioconjugation of quantum dots, Coord. Chem. Rev. 263 (2014) 101–137.
[5] R. Freeman, J. Girsh, I. Willner, Nucleic acid/quantum dots (QDs) hybrid systems for optical and photoelectrochemical sensing, ACS Appl. Mat. Interfaces 5 (2013) 2815–2834.
[6] M. Frasco, N. Chaniotakis, Bioconjugated quantum dots as fluorescent probes for bioanalytical applications, Anal. Bioanal. Chem. 396 (2010) 229–240.
[7] E. Oh, M.Y. Hong, D. Lee, S.H. Nam, H.C. Yoon, H.S. Kim, Inhibition assay of biomolecules based on fluorescence resonance energy transfer (FRET) between quantum dots and gold nanoparticles, J. Am. Chem. Soc. 127 (2005) 3270–3271.
[8] Y. Zhang, X. Ke, Z. Zheng, C. Zhang, Z. Zhang, F. Zhang, Q. Hu, Z. He, H. Wang, Encapsulating quantum dots into enveloped virus in living cells for tracking virus infection, ACS Nano 7 (2013) 3896–3904.
[9] S. Wang, N. Mamedova, N.A. Kotov, W. Chen, J. Studer, Antigen/antibody immunocomplex from CdTe nanoparticle bioconjugates, Nano Lett. 2 (2009) 817–822.
[10] N. Ma, E.H. Sargent, S.O. Kelley, One-step DNA-programmed growth of luminescent and biofunctionalized nanocrystals, Nat. Nanotechnol. 4 (2009) 121–125.
[11] G. Tikhomirov, S. Hoogland, P.E. Lee, A. Fischer, E.H. Sargent, S.O. Kelley, DNA-based programming of quantum dot valency, self-assembly and luminescence, Nat. Nanotechnol. 6 (2011) 485–490.
[12] N. Ma, S.O. Kelley, DNA-based programing of quantum dot properties, WIRES Nanomed. Nanobiotechnol. 5 (2013) 86–95.
[13] C. Zhang, J. Xu, S. Zhang, X. Ji, Z. He, One-pot synthesized DNA–CdTe quantum dots applied in a biosensor for the detection of sequence-specific oligonucleotides, Chem. Eur. J. 18 (2012) 8296–8300.
[14] C. Zhang, X. Ji, Y. Zhang, G. Zhou, X. Ke, H. Wang, P. Tinnefeld, Z. He, One-pot synthesized aptamer-functionalized CdTe:Zn^{2+} quantum dots for tumor-targeted fluorescence imaging in vitro and in vivo, Anal. Chem. 85 (2013) 5843–5849.
[15] Q. Fu, L. Yang, W. Wang, A. Han, J. Huang, P. Du, Z. Fan, J. Zhang, B. Xiang, Synthesis and enhanced electrochemical catalytic performance of monolayer $WS_{2(1-x)}Se_{2x}$ with a tunable band gap, Adv. Mater. 27 (2015) 4732–4738.
[16] D. Voiry, H. Yamaguchi, J. Li, R. Silva, D.C.B. Alves, T. Fujita, M. Chen, T. Asefa, V.B. Shenoy, G. Eda, M. Chhowalla, Enhanced catalytic activity in strained chemically exfoliated WS_2 nanosheets for hydrogen evolution, Nat. Mater. 12 (2013) 850–855.
[17] S. Yu, J.W. Jung, I.D. Kim, Single layers of WS_2 nanoplates embedded in nitrogen-doped carbon nanofibers as anode materials for lithium-ion batteries, Nanoscale 7 (2015) 11945–11950.
[18] Y. Liu, W. Wang, H. Huang, L. Gu, Y. Wang, X. Peng, The highly enhanced performance of lamellar WS_2 nanosheet electrodes upon intercalation of single-walled carbon nanotubes for supercapacitors and lithium ions batteries, Chem. Comm. 50 (2014) 4485–4488.
[19] T. Georgiou, R. Jalil, B.D. Belle, L. Britnell, R.V. Gorbachev, S.V. Morozov, Y.J. Kim, A. Gholinia, S.J. Haigh, O. Makarovsky, L. Eaves, L.A. Ponomarenko, A.K. Geim, K.S. Novoselov, A. Mishchenko, Vertical field-effect transistor based on graphene-WS_2 heterostructures for flexible and transparent electronics, Nat. Nanotechnol. 8 (2013) 100–103.
[20] Q. Xi, D.M. Zhou, Y.Y. Kan, J. Ge, Z.K. Wu, R.Q. Yu, J.H. Jiang, Highly sensitive and selective strategy for MicroRNA detection based on WS_2 nanosheet mediated fluorescence quenching and duplex-specific nuclease signal amplification, Anal. Chem. 86 (2014) 1361–1365.
[21] Y. Yuan, R. Li, Z. Liu, Establishing water-soluble layered WS_2 nanosheet as a platform for biosensing, Anal. Chem. 86 (2014) 3610–3615.
[22] J. Ge, L.J. Tang, Q. Xi, X.P. Li, R.Q. Yu, J.H. Jiang, X. Chu, A WS_2 nanosheet based sensing platform for highly sensitive detection of T4 polynucleotide kinase and its inhibitors, Nanoscale 6 (2014) 6866–6872.
[23] M. Pumera, A.H. Loo, Layered transition-metal dichalcogenides (MoS_2 and WS_2) for sensing and biosensing, Trac Trend Anal. Chem. 61 (2014) 49–53.
[24] J. Zhao, X. Jin, M. Vdovenko, L. Zhang, I.Y. Sakharov, S. Zhao, A WS_2 nanosheet based chemiluminescence resonance energy transfer platform for sensing biomolecules, Chem. Comm. 51 (2015) 11092–11095.
[25] J. Zhao, Y. Ma, R. Kong, L. Zhang, W. Yang, S. Zhao, Tungsten disulfide nanosheet and exonuclease III Co-assisted amplification strategy for highly sensitive fluorescence polarization detection of DNA glycosylase activity, Anal. Chim. Acta 887 (2015) 216–223.
[26] U. Resch-Genger, M. Grabolle, S. Cavaliere-Jaricot, R. Nitschke, T. Nann, Quantum dots versus organic dyes as fluorescent labels, Nat. Meth. 5 (2008) 763–775.
[27] M. Stanisavljevic, S. Krizkova, M. Vaculovicova, R. Kizek, V. Adam, Quantum dots fuorescence resonance energy transfer-based nanosensors and their application, Biosens. Bioelectron. 74 (2015) 562–574.
[28] W.R. Algar, H. Kim, I.L. Medintz, N. Hildebrandt, Emerging non-traditional förster resonance energy transfer configurations with semiconductor quantum dots: investigations and applications, Coord. Chem. Rev. 263 (2014) 65–85.
[29] Z. Wu, Z. Zhen, J.H. Jiang, G.L. Shen, R.Q. Yu, Terminal protection of small-molecule-linked DNA for sensitive fluorescence detection of protein binding based on nucleic acid amplification, J. Am. Chem. Soc. 131 (2009) 12325–12332.
[30] Y. Cao, S. Zhu, J. Yu, X. Zhu, Y. Yin, G. Li, Protein detection based on small molecule-linked DNA, Anal. Chem. 84 (2012) 4314–4320.
[31] Y. He, X.J. Xing, H.W. Tang, D.W. Pang, Graphene oxide-based fluorescent biosensor for protein detection via terminal protection of small-molecule-linked DNA, Small 9 (2013) 2097–2101.
[32] C.H. Chen, X. Xiang, Y.F. Liu, G.H. Zhou, X.H. Ji, Z.K. He, Dual-color determination of protein via terminal protection of small-molecule-linked DNA and the enzymolysis of exonuclease III, Biosens. Bioelectron. 58 (2014) 205–208.
[33] J. Zhuang, X. Zhang, G. Wang, D. Li, W. Yang, T. Li, Synthesis of water-soluble ZnS : Mn^{2+} nanocrystals by using mercaptopropionic acid as stabilizer, J. Mater. Chem. 13 (2013) 1853–1857.
[34] M. Chakraborty, F.W. Hsiao, B. Naskar, C.H. Chang, A.K. Panda, Surfactant-assisted synthesis and characterization of stable silver bromide nanoparticles in aqueous media, Langmuir 28 (2012) 7282–7290.
[35] X. Huang, S. Neretina, M.A. El-Sayed, Gold nanorods: from synthesis and properties to biological and biomedical applications, Adv. Mater. 21 (2009) 4880–4910.
[36] S. Xu, D. Li, P. Wu, One-pot, facile, and versatile synthesis of monolayer MoS_2/WS_2 quantum dots as bioimaging probes and efficient electrocatalysts for hydrogen evolution reaction, Adv. Funct. Mater. 25 (2015) 1127–1136.
[37] N. Ma, G.A. Tikhomirov, S.O. Kelley, Nucleic acid-passivated semiconductor nanocrystals: biomolecular templating of form and function, Acc. Chem. Res. 43 (2010) 173–180.
[38] J. Aldana, N. Lavelle, Y. Wang, X. Peng, Size-dependent dissociation pH of thiolate ligands from cadmium chalcogenide nanocrystals, J. Am. Chem. Soc. 127 (2005) 2496–2504.
[39] S. Celebi, A.K. Erdamar, A. Sennaroglu, A. Kurt, H.Y. Acar, Synthesis and characterization of poly(acrylic acid) stabilized cadmium sulfide quantum dots, J. Phys. Chem. B 111 (2007) 12668–12675.
[40] L.J. Sang, H.F. Wang, Aminophenylboronic-acid-conjugated polyacrylic acid–Mn-doped ZnS quantum dot for highly sensitive discrimination of glycoproteins, Anal. Chem. 86 (2014) 5706–5712.
[41] P. Wang, Z. Xia, J. Yan, X. Liu, G. Yao, H. Pei, X. Zuo, G. Sun, D. He, A study of pH-dependence of shrink and stretch of tetrahedral DNA nanostructures, Nanoscale 7 (2015) 6467–6470.
[42] C.H. Chen, X. Xiang, Y.F. Liu, G.H. Zhou, X.H. Ji, Z.K. He, Dual-color determination of protein via terminal protection of small-molecule-linked DNA and the enzymolysis of exonuclease III, Biosens. Bioelectron. 58 (2014) 205–208.

Please cite this article in press as: C. Zhang, et al., One-step synthesis of DNA functionalized cadmium-free quantum dots and its application in FRET-based protein sensing, Analytica Chimica Acta (2016), http://dx.doi.org/10.1016/j.aca.2016.12.024